JMEPEG (2004) 13:218–225
DOI: 10.1361/10599490418424

1059-9495/$19.00

Quantitative Evaluation of Fracture Toughness–Microstructural Relationships in Alpha-Beta Titanium Alloys

N.L. Richards

(Submitted 21 July 2003; in revised form 9 January 2004)

The fracture toughness of two alpha-beta titanium alloys containing an alpha platelet in a transformed beta matrix has been examined in terms of the microstructural parameters controlling the fracture initiation and propagation in the alloys. Equations have been formulated that show that the highest toughness values of both alloys were associated with the finest platelet spacings and the thickest alpha platelets. It is proposed that the fracture initiation process in both alloys is controlled by the distance between the platelets, the fracture toughness of the alloys being dependent on the distance between active centers of void nucleation, i.e., as a function of the alpha platelet thickness and spacing between the platelets. Seven models of ductile fracture relating fracture toughness to mechanical property and microstructural parameters have been compared in their ability to predict the toughness of the alloys after solution treatments, which produce varying platelet thickness and inter-platelet spacings. The principle has been adopted following Rice and Rosengren and Hutchinson (HRR)[1,2] that there must be a 1/*x* energy singularity at the crack tip, which also prescribes the stress and strain distribution ahead of a crack tip. Any model not incorporating these requirements should be rejected.

Keywords alpha-beta titanium alloys, fracture toughness, platelet spacings

1. Introduction

Previous research by Margolin et al.[3] showed that fracture strength values of three alpha-beta titanium alloys with equiaxed and Widmanstatten plus continuous alpha could be related to the size, morphology, and location of the alpha grains and the size of the beta grains. Fentiman et al.[4] showed that the fracture toughness of acicular structures in a Ti/11Sn/2.25A//4Mo/0.25Si alloy was superior to the equiaxed material for strengths up to 1240 MPa (180 k.s.i.). Similarly the toughness and microstructure of alloy Ti/6Al/4V and in two alpha/beta titanium alloys showed an increase in toughness of 40% and up to 100%, achieved with little reduction of strength, by incorporating a platelet alpha into a transformed beta matrix.[5,6]

The variation of strain ε ahead of a crack has been evaluated by a number of authors. In the elastic case, ε varies as $x^{-1/2}$, while in thin metal plates Gerberich[7] found an x^{-1} to $x^{-1/2}$ variation depending on the plastic zone size and the value of n (see Appendix for symbols used). Rice[8] has shown a similar singularity in torsion with strain again depending on n, while Neimark[9] found that ε varied approximately as x^{-1} for low n values. Similarly Dixon[10] observed an x^{-1} strain distribution ahead of a crack. Rice and Johnson[11] have shown that values of ε from 0.1 to 2.0 are usually possible in the heavily deformed region ahead of a crack up to a distance of about 1.9 δ, where δ is the crack opening displacement. It seems probable therefore that the elastic solution should not be used to describe the variation of ε ahead of a crack in a material failing in a ductile manner and that one should use an x^{-1} dependence suitably modified by the appropriate work hardening coefficient.

N.L. Richards, Department of Mechanical & Industrial Engineering, University of Manitoba, Winnipeg, MB, Canada R3T 5V6. Contact e-mail: nrichar@cc.umanitoba.ca.

Nomenclature

x	distance ahead of crack tip
K_{1c}	plane strain fracture toughness
λ_α	alpha platelet thickness
λ_β	interplatelet spacing
f	volume fraction of phase
N_L	number of intercepts per unit length
r	correlation coefficient
f_1/f_2	functions of microstructural parameter
E	Young's modulus
dT	microstructural parameter in Krafft equation
n	work hardening coefficient in Ludwik equation
N	work hardening parameter in the Ramsberg-Osgood equation
l	microstructural parameter
σ_{ys}	yield strength
r_c	crack tip radius
ε_i	strain to instability
ε	true fracture strain
ε_c	critical true fracture strain
ν	Poisson's ratio
δ	crack tip COD
δ_c	critical crack tip COD
D	diameter of void or second phase particle

For small-scale yielding it has been established by Rice and Rosengren[1] and Hutchinson[2] that the strain distribution ahead of a stationary crack tip, is

$$\varepsilon_{ij} = \alpha\varepsilon_o\left[\frac{J}{\alpha\sigma_{ys}\varepsilon_o I_n r}\right]^{N/N+1} u(\theta) \quad \text{(Eq 1)}$$

where α and I_n are constants obtained from Ref 1; ε_o is the flow stress; J is Rice's contour integral; σ_{ys} is the yield stress; N is the strain hardening coefficient in the Ramberg-Osgood equation, equal to $1/n$, the strain hardening exponent in the Ludwik equation; and u (θ) is a constant depending on the angular position and N, also obtained from Ref. 1.

For a given material, $\varepsilon_{ij\,\alpha}\,(J/r)^{N/N+1}$ and with $N > 13$, $N/(N+1)$ is approximately 1. Therefore, $\varepsilon_{ij\,\alpha}\,(\delta/r)$ with $J = \sigma_{ys}\delta$.

Thus the strain exhibits at the crack tip a $1/r$ singularity. In the linear elastic region, from Irwin's research[12] on the stress intensity factor K, the existence of the $1/r^{1/2}$ dominant term close to the crack tip is well known.

The present work was aimed at a quantitative investigation of the microstructural features controlling the fracture toughness. Measurements have been made of volume fractions of alpha and beta, mean free path between the phases, and void volume fraction using standard stereological techniques. These measurements were then correlated with the plane strain fracture toughness of the alloys K_{1c} to determine the main factors controlling the toughness. Finally the quantitative stereological parameters and the mechanical properties of the alloys were used to compare the ability of quantitative models of ductile fracture in predicting the fracture toughness of the alloys.

2. Experimental

The alloys studied were Ti/6Al/5Zr/4Mo/1Cu/0.2Si (Alloy A) and Ti/6Al/4V (Alloy B). The composition of the alloys is given in Table 1. Alloy A (beta transus 995 °C) was received in the form of a 4 in. square billet and had been solution treated at 900 °C, air cooled (AC) and aged at 500 °C for 24 h. Alloy B (beta transus 1015 °C) was of similar dimension but was in the as-forged condition.

Further forging was carried out isothermally on both alloys at 950, 1050, and 1125 °C, with forging reductions of about 70%. Blanks were cut from the forged pancakes and given the following double heat treatment (DHT):

1) Alloy A: Heated to 1040 °C for 1 h and cooled at an average rate of 100 °C/h to 675 °C to precipitate out a substantial amount of the alpha phase. Solution treatment was carried out at 800, 900, and 950 °C for 1 h and then air-cooled. Aging was carried out at 500 °C for 24 h. Further blanks were processed in the same manner, but oil quenched (OQ) after solution treatment and aged as above.
2) Alloy B: Heated to 1040 °C for 1 h and cooled at an average rate of 100 °C/h to 675 °C. Solution treatment was carried out at 800, 875, and 950 °C for 1 h, water quenched followed by aging at 510 °C for 8 h.

Table 1 Chemical Composition of Alloys in Weight Percent

Alloy	Elements, wt.%					
Alloy A	Al	V	Fe	C	O	N
	6.15	3.97	0.08	0.03	1800 ppm	82 ppm
Alloy B	Al	Zr	Mo	Cu	O	Si
	6.0	5.0	4.0	1.0	1200 ppm	0.2

Approximately 2.54 mm (0.1 in.) was machined off all faces of the blanks as part of the test pieces preparation and checked by hardness measurements to ensure removal of any oxide.

Fracture toughness testing was carried out using an Instron machine in accordance with ASTM E399 requirements using three-point bend specimens with a specimen/width ratio of 4:1. Fatigue cracking of the notches was carried out such that the last 1.27 mm (0.050 in) of the crack propagated in greater than 50,000 cycles at a stress intensity range of less than 50% of K_{1c}.

Three specimens were tested at each solution temperature, two to evaluate the fracture toughness and one for metallographic use. This specimen was polished and etched at the base of the notch and etched prior to fatigue cracking. Etching was carried out using Kroll's reagent (2% Hf/10% HNO_3/88% water). Where necessary, further etching in 0.5% HF in water was used to emphasize the structure of the transformed beta. All the fracture toughness values used in the present work are valid using the ASTM criterion in E399.

Measurements of the alpha platelet thickness (λ_α) and the interplatelet spacing (λ_β) were made on an image analyzer. Measurements were made from 40 fields for three forging temperatures and three solution treatment temperatures. The values of λ_α and λ_β were calculated from Fullman's mean free path formula,[13] using the f and N_L values determined on the image analyser. Fullman showed that

$$\lambda = (1 - f)/N_L$$

where f is the volume fraction of the phase and is equal to N_L, the number of intercepts per unit length, i.e.,

$$\lambda_\alpha = (1 - f_\beta)/N_L \text{ and } \lambda_\beta = (1 - f_\alpha)/N_L:$$

where N_L is the same for both λ_α and λ_β.

During fracture toughness testing, voids were generated within the plastic zone ahead of the crack tip. Void volume fraction f measurements and the number of voids per unit length, N_{LV} for Alloy A were measured on a scanning electron microscope (SEM) using approximately 1000 points for the volume fraction measurements.

The fractions of voids generated within the plastic zone of Alloy B were approximately an order of magnitude less than the values measured in Alloy A. Thus sufficient numbers of voids could not be measured to enable a reasonably accurate volume fraction to be quoted.

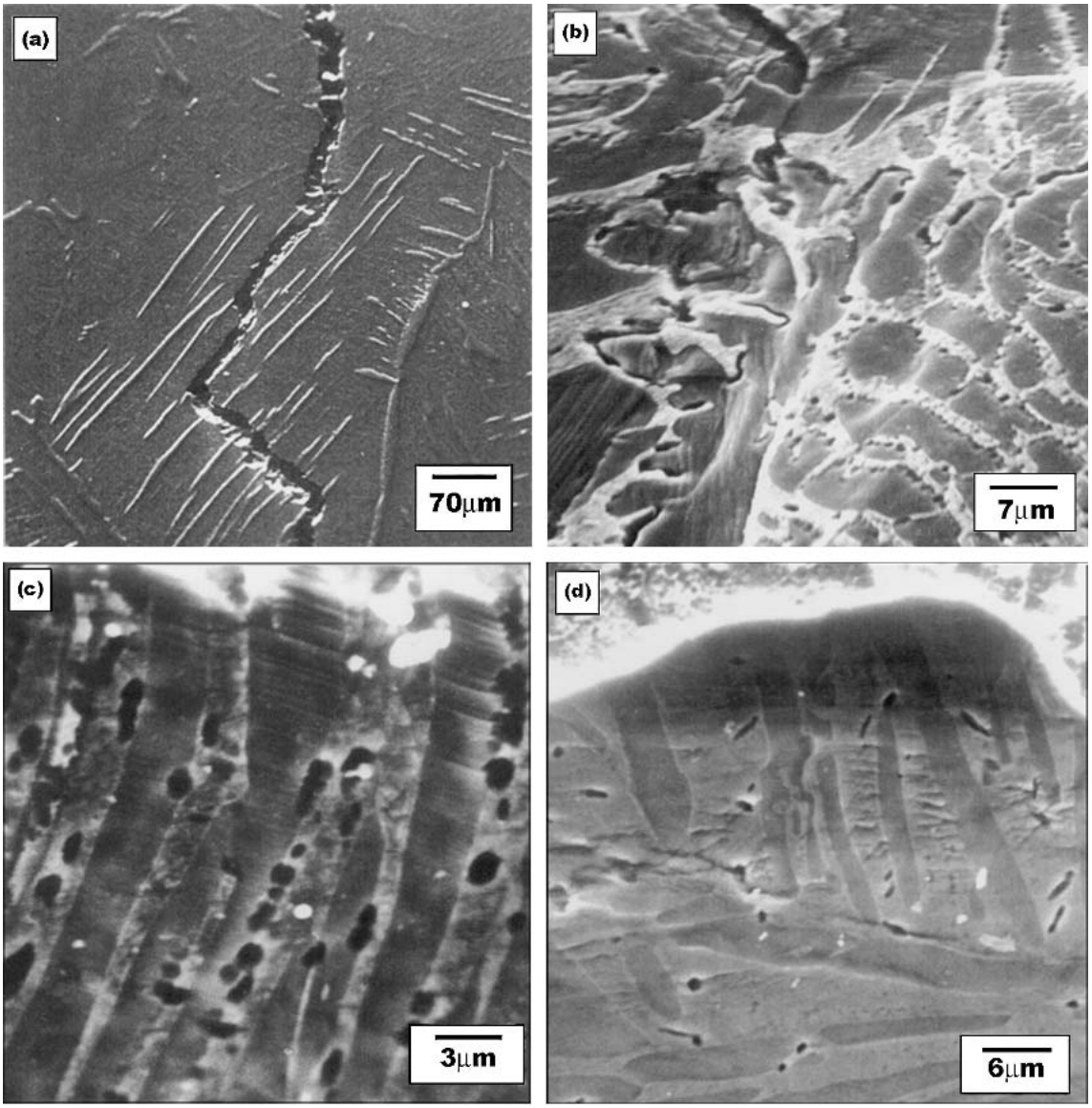

Fig. 1 SEM micrographs of cracks in plastic zone: **(a)** crack deflecting around alpha platelets in Alloy B, **(b)** crack deviating around alpha platelets in Alloy A, **(c)** crack propagating through alpha platelets and slip lines visible in alpha in Alloy A, **(d)** crack propagation and void formation in plastic zone of Alloy A

3. Results

3.1 Void Nucleation in Plastic Zone

Voids were mainly nucleated within the plastic zone of both alloys at the platelet alpha transformed beta interfaces, though the fraction of voids in alloy B was an order of magnitude less than that in Alloy A. If the energy to fracture the alpha platelets was greater than that involved in circumventing the alpha colony, then the crack would deviate past the colony as shown in Fig. 1(a) for alloy B and around platelets in alloy A (Fig. 1b); otherwise the crack would cut across alpha platelets (Fig. 1c and 1d). In both alloys, the failure mechanism is one of void formation ahead of the crack and linking up of voids with the main crack.

Quantitative measurements of the percentage of voids within the plastic zone was possible for only Alloy A due to the low percentage of voids in the tougher alloy (B).

Figure 2 shows the fracture toughness/percentage voids (f) relationship, and the best fit to the data obtained using an equation of the form, $K_{1c} = cf^{-d}$, where c and d are constants, gave $K_{1c} = 64.6\, f^{-0.45}$ with $r = 0.73$ significant at the 5% level.

3.2 Relationships Between K_{1c} and Microstructural Parameters

Graphs of K_{1c} against λ_α for both alloys were found to obey straight-line relationships whether plotted directly or against the square root of the microstructural parameter, the toughness increasing with increasing alpha platelet thickness. Figures 3(a) and 3(b) show the variation of K_{1c} with λ_α for both alloys.

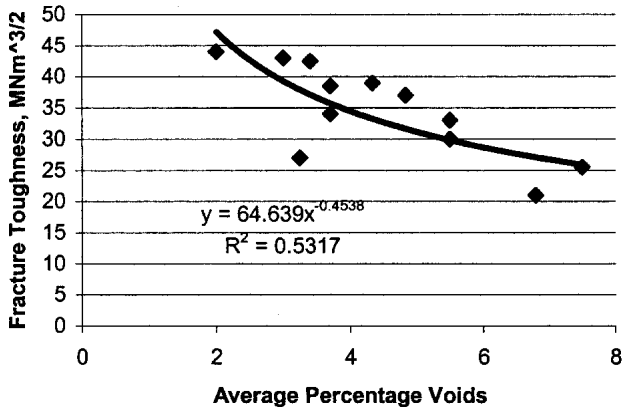

Fig. 2 Fracture toughness versus percentage voids in plastic zone

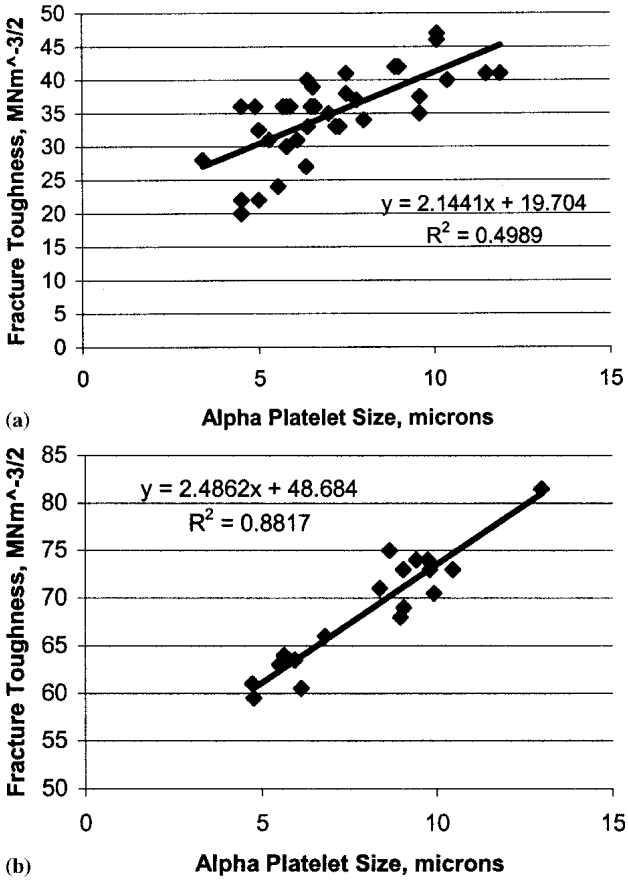

Fig. 3 Variation of fracture toughness with alpha platelet spacing: **(a)** fracture toughness versus alpha platelet size for Alloy A, **(b)** fracture toughness versus alpha platelet size for Alloy B

Regression analysis for the above-mentioned relationships gave

Alloy A: $K_{1c} = 19.3 + 2.2\,\lambda_\alpha$
correlation coefficient $r = 0.70$
$K_{1c} = 4.7 + 11.4\,\lambda_\alpha^{1/2}$
correlation coefficient $r = 0.68$
35 Degrees of Freedom

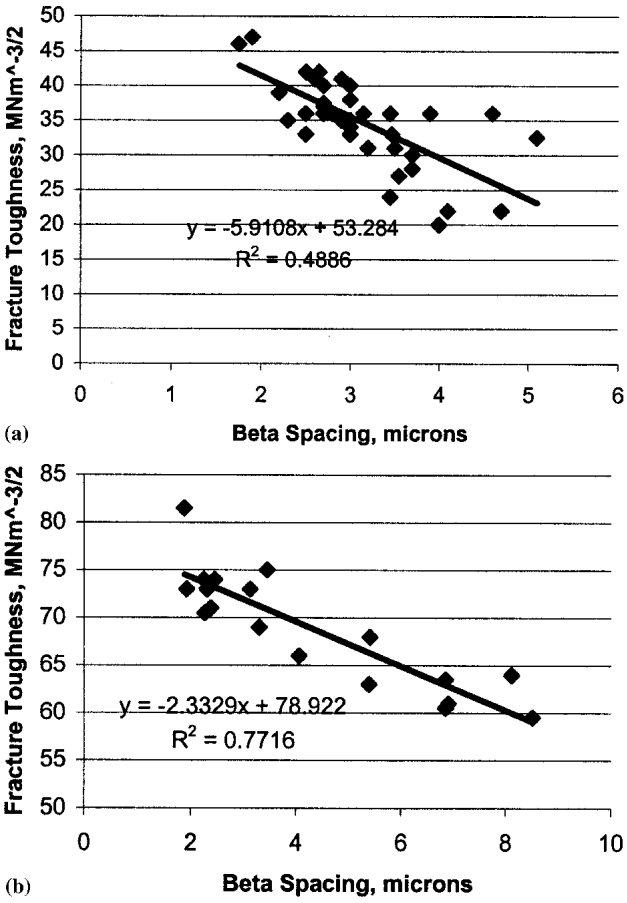

Fig. 4 Variation of fracture toughness with beta spacing: **(a)** fracture toughness versus beta spacing for Alloy A, **(b)** fracture toughness versus beta spacing for Alloy B.

Alloy B: $K_{1c} = 48.7 + 2.5\,\lambda_\alpha$
correlation coefficient $r = 0.94$
$K_{1c} = 29.7 + 13.9\,\lambda_\alpha^{1/2}$
correlation coefficient $r = 0.94$
16 Degrees of Freedom
K_{1c} is in $MNm^{-3/2}$ and the platelet thickness in microns.

The toughness of both alloys was found to increase with decreasing distance between the alpha platelets λ_β, as shown in Fig. 4(a) and 4(b) for Alloys A and B, respectively. Regression analysis showed that the best fit for the data was given by the following equations:

Alloy A: $K_{1c} = 15.4 + 57.5\,\lambda_\beta^{-1}$
correlation coefficient = 0.73
$K_{1c} = 2.15\,\lambda_\beta^{-1/2} - 4.47$
correlation coefficient = 0.735
35 Degrees of Freedom

Alloy B: $K_{1c} = 57.6 + 37.3\,\lambda_\beta^{-1}$
correlation coefficient = 0.88
$K_{1c} = 47.5 + 1.27\,\lambda_\beta^{-1/2}$
correlation coefficient = 0.89
16 Degrees of Freedom

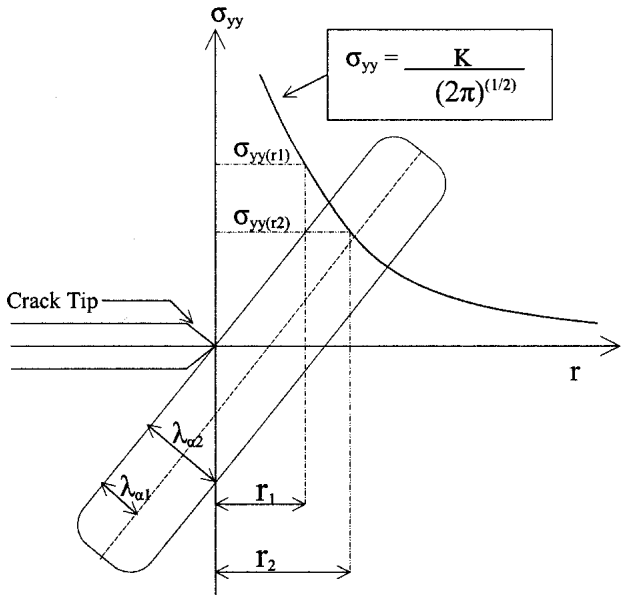

Fig. 5 Schematic representation of an alpha platelet at 45° to crack tip

An attempt was also made to use the two microstructural parameters in a multiple linear regression analysis (MLRA) to predict the fracture toughness of the alloys from one equation, i.e.,

$$K_{1c} = f_1\lambda_\alpha{}^a \pm f_2\lambda_\beta{}^b$$

Examination of the matrix correlation data, however, showed an inter-relationship between the λ_α and λ_β parameters, and consequently the MLRA approach was disregarded.

4. Discussion

4.1 Microstructural Effects in Plastic Zone

Figure 1(a) and (b) show deflection of the crack by the alpha platelets and Fig.1(c) and (d) show the shearing and slip associated with cutting of the alpha platelet. Qualitatively, therefore, from the microstructural and statistical evidence, the fracture toughness is controlled by the size (thickness) of the alpha phase and the spacing between adjacent alpha platelets (the thickness of the beta phase). If one envisages a series of alpha platelets inclined at an angle of 45° to the stress axis (Fig. 5), a crack running into the alpha phase would cut the platelet at $\sqrt{2\lambda_\alpha}$ if energetically favorable. The stress intensity at $\lambda_{\alpha 1}$ will be greater than at $\lambda_{\alpha 2}$ as $K\alpha\sigma(2\pi r)^{1/2}$ and σ_{yyr1} is greater than σ_{yyr2}. With voids being formed generally on one side of an alpha platelet at the alpha/beta interface, the next possible interface from an existing alpha/beta combination is $\sqrt{2(\lambda_\alpha + \lambda_\beta)}$. In the tougher alloy B, the microstructural parameter could also be a multiple of this value, though for alloy A the $\sqrt{2(\lambda_\alpha + \lambda_\beta)}$ factor is the most likely from microstructural observations. Thus in any relationship between fracture toughness and a microstructural unit, functions of the $\sqrt{2(\lambda_\alpha + \lambda_\beta)}$ relationship would likely be applicable. Therefore the spacing and alpha platelet thickness are important in determining the toughness of the alloys, with voids that had been nucleated at the alpha platelet-transformed beta interfaces constrained by the alpha spacing. Thus cracks growing with fine alpha platelet spacing are less likely to grow than those with a coarse spacing. It should be noted that Greenfield and Margolin[3] did not observe voids at alpha platelet-transformed beta interfaces, only finding voids at grain boundary alpha interfaces.

4.2 Models Relating Fracture Toughness to Microstructure

Several models have been developed to relate the microstructural and mechanical properties of an alloy to its fracture toughness K_{1c}, though some of them are not well designed for experimental verification. The results from the previous section were used to assess the suitability of the models in predicting the toughness of the double heat treatment (DHT) titanium alloys with a view to elucidating the mechanical and microstructural parameters that control the toughness in this heat treated condition. The models used are shown below:

1. Krafft[14]

$$K_{1c} = En(2\pi d_T)^{1/2}$$

The equation is based on the elastic solution; E is Young's Modulus and d_T is a microstructural parameter.

2. Thomason[15]

$$\frac{K_{1c}}{Y} = \left\{\Gamma_c\left[4.62(E/Y)\frac{e^{\varepsilon_{i-1}}}{1-\nu^2} + 8.81\tan\left(\frac{\pi}{2}\left(1-\frac{V_f}{0.09}\right)\right)\right]\right\}^{1/2}$$

The equation is limited to volume fractions from 2% to 9%. The present author has used the percentage voids in plastic zone for the V_f value. The work-hardening coefficient is equated to ε_I, and one also has to estimate r_c (taken as 0.0000127 m). $Y = \sqrt{3}k$, where k = shear yield stress.

3. Hahn and Rosenfield[16]

$$K_{1c} = n(2/3E\sigma_{ys}\varepsilon)^{1/2}$$

There is no microstructural factor directly in equation, but a microstructural factor l is related to n, as l is proportional to n^2.

4. Broberg[17]

$$K_{1c} = 3\left[Ed\,\sigma_{ys}\left(\frac{\varepsilon_m}{1-\varepsilon_m}\right)\right]^{1/2}$$

where ε_m is the reduction in area and has been equated in the present context to the true fracture strain ε_c

5. Schwalbe[18]

$$K_{1c} = [\sigma_{ys}/(1-2\nu)] \sqrt{\{\pi d(1+n) \cdot [\varepsilon_B E/\sigma_{ys}]^{1+n}\}}$$

ε_B has been equated to n by the present author.

6. Hahn and Rosenfield[19]

$$K_{1c} = (2\sigma_{ys} E d)^{1/2}$$

7. Richards

$$K_{1c} = \frac{\pi}{2}\left(\frac{E\, w_{(n)}\sigma_{ys}\varepsilon_c 1_c}{(1-\nu^2)}\right)^{1/2}$$

As shown above in Fig. 1(a-d), the presence of the acicular alpha/beta microstructure makes the fracture path more tortuous, and hence, the alloys tougher via deflection of the crack away from the x axis. To develop a fracture toughness–microstructural model to explain the present results, one can adapt Wells' relationship[20] between the strain energy release rate G and the crack tip crack opening displacement δ as follows:

$$G = (\pi/4)\sigma_{ys}\delta \quad \text{(Eq 2)}$$

under plane strain conditions and noting that $K_{1c}{}^2 = EG_{1c}$:

$$(1-\nu^2)K_{1c}{}^2/E = G_{1c} \quad \text{(Eq 3)}$$

and

$$(\pi/4)\sigma_{ys}\delta_c = (1-\nu^2)K_{1c}{}^2/E \quad \text{(Eq 4)}$$

However, Wells,[20] Cottrell,[21] and the HRR strain relationship have showed that

$$\delta = \pi\varepsilon l \quad \text{(Eq 5)}$$

where ε is the strain and l is the distance ahead of crack tip. Substituting Eq 5 into Eq 4 at crack extension gives

$$K_{1c} = \frac{\pi}{2}\left(\frac{E\,\sigma_{ys}\varepsilon l}{(1-\nu^2)}\right)^{1/2} \quad \text{(Eq 6)}$$

In plane strain, however, the yield stress is augmented above the yield value depending on n, the work hardening coefficient.[22] If this augmentation of stress is $w_{(n)}$, insertion into Eq 6 gives

$$K_{1c} = \frac{\pi}{2}\left(\frac{E w_{(n)}\sigma_{ys}\varepsilon l}{(1-\nu^2)}\right)^{1/2} \quad \text{(Eq 7)}$$

If we equate ε to the tensile true strain in uniaxial tension ε_c and $l = l_c$ the critical microstructural unit ahead of the crack tip, Eq 6 becomes

$$K_{1c} = \frac{\pi}{2}\left(\frac{E w_{(n)}\sigma_{ys}\varepsilon l_c}{(1-\nu^2)}\right)^{1/2} \quad \text{(Eq 8)}$$

A similar equation without the $(\pi/2)$ constant has been developed by Ritchie and Thompson[23] from a J integral approach (Eq 1), also without the incorporation of the work hardening effect $w_{(n)}$, in the plastic zone and with ε being a likely function of fracture surface micro-roughness and volume fraction of void initiation particles, rather than the true fracture strain in tension. Similarly one can also evaluate an equation of a form similar to Eq 8 from Goodier and Field's analysis for δ_c.[24] In this case, only the numerical factor at the front of Eq 8 would differ; the other parameters would remain the same.

The proportional relationship of K_{1c} and σ_{ys} at first would seem incorrect, as the normal relationship is an inverse one. In the present context it is interpreted as a K_{1c}-toughness relationship with the $(\sigma_{ys.}\varepsilon_c)$ product being interpreted as a function of the toughness of an alloy. Precedence for this is the definition of toughness or the area under the stress-strain curve (i.e., the product of a function of stress multiplied by the strain).

The majority of research papers at present use finite element analysis (FEA) based on limited void growth ahead of a crack tip, or the variation due to Gurson.[25] As Pardoen and Hutchison[26] have pointed out recently in these FEA models, the microstructure of the alloy is inadequately represented. The present model (Eq 8) above, however, takes microstructural and mechanical features into consideration and also satisfies the comments made by Wilsdorf[27] in supplying a simple equation based on few factors, easily obtained from tensile data, coupled with an appropriate microstructual factor. In the present context, the microstructural factor is a function of the thickness of the alpha platelets and their spacing, whereas for steel the factor would likely be the inclusion spacing(s) and for aluminum alloys, the intermetallic spacing(s).

The best fit with the experimental data for models 3, 4, and 7 was found by equating the true strain at fracture from tensile data with the critical value of the true strain ε_c.

The values of the microstructural unit in models 1, 4, 5, 6, and 7 have been initially equated in the present situation to that of $\sqrt{2}$ times the thickness of the alpha platelet. This assumes the average case to be where a platelet meets a crack at an angle of 45°.

The calculated K_{1c} values along with the values of the parameters used in the equations are compared with the experimentally determined values in Table 2. For alloy A, the models of Krafft, Thomason (with $r_c = 0.0000127$ m), Broberg, and the present authors gave the best fit to the measured K_{1c} values.

All the models were found to predict low fracture toughness values for alloy B when using $\sqrt{2(\lambda_\alpha + \lambda_\beta)}$ for the microstructural d value. Consequently this factor was replaced by $\sqrt{2(2\lambda_\alpha + \lambda_\beta)}$; i.e., this assumes the critical microstructural unit to be two alpha platelets apart since the void content inthe alloy is considerably less than in alloy A. Using this approach Table 2 shows that for alloy B, models 1, 4, 6, and 7 predicted the experimental toughness values reasonably well.

Table 2 Calculations for Fracture Toughness-Microstructural Models

Fracture Toughness $MNm^{-3/2}$	YS, MN/m^2	Critical Micro-structural Unit, m $\sqrt{2(\alpha+\beta)}$	Work Hardening Coefficient	$w(n)$	Mean Vol Frac. Voids	True Fracture Strain in Uniaxial Tension	Calculated Fracture Toughness, $MN/m^{-3/2}$						
							Krafft	Thomason	Hahn & Rosenfield	Broberg	Schwalbe	Hahn & Rosenfield	Richards
Alloy A													
20	1285	0.00001074	0.035	2.7	0.083	0.083	32	17	98	35	52	55	29
25	1259	0.0000116	0.035	2.7	0.083	0.083	33	17	97	36	54	57	30
30	1234	0.0000126	0.035	2.7	0.065	0.106	34	18	109	43	63	59	35
35	1208	0.00001357	0.04	2.8	0.038	0.108	41	24	124	44	66	60	37
40	1183	0.000015	0.04	2.8	0.023	0.128	43	24	134	51	75	63	42
45	1157	0.0000168	0.04	2.8	0.015	0.142	45	27	139	57	83	66	46
Alloy B		$\sqrt{(2\alpha+\beta)}$											
60	1050	0.0000243	0.045	2.875	insuffient	0.163	61	insufficient	160	70	103	75	57
65	1000	0.0000277	0.045	2.875	data	0.163	66	data	156	73	108	78	59
70	951	0.0000317	0.055	2.98		0.163	86		186	76	115	82	63
75	944	0.0000348	0.055	2.98		0.174	90		191	82	124	85	68
80	941	0.0000382	0.055	2.98		0.2	94		205	94	140	89	76

Thomason's model could not be used for alloy B since, as mentioned previously, the percentages of voids are well below the 2% minimum value required by the equation.

A number of the models predict that K_{1c} is proportional to the square root of the microstructural parameter, though one has to define the appropriate relationship for a particular alloy. This is in general agreement with the regression equations developed earlier, where it was shown that it was not generally possible to distinguish between the K_{1c}/λ_α or $\lambda_\alpha^{1/2}$ relationships in the present case.

Similarly, with λ_α proportional to λ_β^{-1}, K_{1c} will be a function of λ_β, which is again predicted by the regression analysis. The research showed that voids were initiated at the alpha platelet/matrix interface and were constrained from growing by the spacing between the platelets λ_β until the voids grew into and finally through the platelets. The λ_β spacing will thus control the void initiation and initial growth processes, while the toughness of the alloys will be controlled by the spacing between the voids (function of λ_α), since fracture toughness is concerned with crack propagation, i.e., void linkage. In alloy A the minimum void spacing will be a function of the alpha platelet thickness and a multiple of the thickness in alloy B.

Though a number of the models appear to reasonably predict the toughness of the alloys, it is not possible to clearly distinguish between them in predicting the toughness of the two alloys over the whole toughness range due to the inherent scatter in measurements of the structural parameters.

One may further distinguish between the various models on the basis of their derivation. In principle, ahead of the crack tip there must be a $1/x$ singularity for the product of stress and strain as proposed by Dixon,[10] Rice and Rosengren,[1] and Hutchinson.[2] Consequently, the stress and strain distributions are also as prescribed by Rice and Rosengren and Hutchinson and any model not consistent with these ideas should be rejected or modified to agree with the above requirements. In the present context it has been assumed that the critical event for ductile crack propagation is the attainment of a critical strain (with ε proportional to $1/x$) in the plastic zone ahead of the crack tip. Models of ductile fracture based on the elastic solution are therefore considered inappropriate by the present author, even though they may show successful empirical relationships with the experimental results. In such cases the parametric relationships should be preserved, but the relationships viewed as empirical unless more appropriate and realistic models can be created fitting the successful empirical equation. Finally it is of interest to note that substitution of l in Model 7 by relationship $l = (\pi/6f)^{1/3} \times D$ leads to K_{1c} proportional to $f^{-1/6}$, i.e., at constant strength and D values. This is the same observation as that found by Hahn and Rosenfield.[19]

5. Conclusions

Regression equations have been developed relating the fracture toughness to the interplatelet spacing λ_β and platelet thickness λ_α of two alpha/beta Ti alloys containing an alpha platelet in a transformed beta matrix.

An attempt to relate both platelet spacing and thickness to toughness using a multiple linear regression analysis was unsuccessful due to an inverse relationship between the platelet thickness and spacing.

Quantitative measurements of the void fractions f within the plastic zone of one of alloys showed $K_{1c} = 64.6f^{-0.45}$. Accurate void fraction measurements were not possible for the second tougher alloy (B), since the void fractions were approximately an order of magnitude less than the other alloy. This result supports the generally observed conclusion that tough materials have fewer voids generated within the plastic zone than less tough alloys.

Seven simple models of toughness-ductile failure were used in an attempt to predict the toughness of the two alloys from their mechanical and microstructural parameters. The models generally agree that the toughness of the alloys is controlled by the modulus and strength parameter, the true fracture strain, work hardening coefficient and a microstructural parameter.

In the two alloys the toughness is a function of the distance between the platelets and the active centers of void nucleation, i.e., a function of the thickness of the alpha platelets.

Following the theories of Rice and Rosengren, and Hutchinson, ductile fracture models are rejected when they do not exhibit a $1/x$ energy singularity ahead of a crack, tip. This also preconditions the stress and strain distributions ahead of a crack.

References

1. J.A. Rice and G.F. Rosengren: "Plane Strain Deformation Near a Crack Tip in a Power-Law Hardening Material," *J. Mech. Phys. Solids,* 1968, *16,* pp. 1-12.
2. J.W. Hutchinson: "Singular Behaviour at the End of a Tensile Crack in a Hardening Material," *J. Mech. Phys. Solids* 1968, *16,* pp. 13-31.
3. H. Margolin, P.A. Farrar, and M.A. Greenfield: "Thermo-Mechanical Strengthening of Titanium Alloys" in *The Science, Technology and Application of Titanium*, R.I Jaffee and N.E.Promisel, ed., Pergamon, NY, 1970, pp. 795-808.
4. W.P. Fentiman, R.E. Goosey, R.J.T. Hubbard, and M.D Smith.: "Exploitation of a Simple Alpha Titanium Alloy in the Development of Alloys of Diverse Mechanical Properties" *The Science, Technology and Application of Titanium*, R.I Jaffee and N.E.Promisel, ed., Pergamon, NY, 1970, pp. 987-99.
5. W.W. Gerberich and G.S. Baker: "Toughness of Two-Phase 6Al-4V Titanium Microstructures" in *Applications Related Phenomena in Titanium Alloys,* ASTM STP 452, ASTM, West Conshocken, PA, 1967, pp. 80-99.
6. N.L. Richards and J.T. Barnby: "The Relationship Between Fracture Toughness and Microstructure in Alpha-Beta Titanium Alloys," *Mater. Sci. Eng.,* 1976, *26*(2), pp. 221-29.
7. W.W. Gerberich: "Plastic Strains and Energy Density in Cracked Plates," *Exp. Mech.*, 1964, Nov., pp. 335-51.
8. J.R. Rice: "Stresses Due to a Sharp Notch in a Work-Hardening Elastic-Plastic Material Under Longitudinal Shear," *J. Appl. Mech.*, 1967, *34,* pp. 287-98.
9. J.E. Neimark: "The Fully Plastic, Plane-Strain Tension of a Notched Bar," *J. Appl. Mech.,* 1968, *35,* pp. 111-16.
10. J.R. Dixon: "Stress and Strain Distributions Around Cracks in Sheet Materials Having Various Work-Hardening Characteristics," *Int. J. Fracture Mech.,* 1965, *1,* pp. 225-44.
11. J.R. Rice and M.A. Johnson: "The Role of Large Crack Tip Geometry Changes in Plane Strain Fracture" in *Inelastic Behaviour of Solids,* M.F Kannenen W.F. Adler, and R.I. Jaffee, ed., McGraw Hill, New York, 1970, pp. 641-70.
12. G.R. Irwin: "Analysis of Stress and Strains Near the End of a Crack Traversing a Plate," *J. Appl. Mech.,* 1957, *79,* pp. 361-64.
13. R.L. Fullman, ''Measurement of Particle Size in Opaque Bodies," *Trans. Am. Inst. Min. Metall. Petrol. Eng.,* 1953, *197,* pp. 447-52.
14. J.M. Krafft and J.H. Mulherin: "Tensile-Ligament Instability and the Growth of Stress-Corrosion Cracks in High-Strength Alloys," *Trans. ASM,* 1969, *62,* pp. 64-80.
15. P.F. Thomason: "A Theoretical Relation Between Fracture Toughness and Basic Material Properties," *Int. J. Fracture Mech.,* 1971, *7*(4), pp. 409-19.
16. G.T. Hahn and A.R. Rosenfield: "Sources of Fracture Toughness: The Relation Between K_{1c} and the Ordinary Tensile Properties of Metals" in *Applications Related Phenomena in Titanium Alloys,* ASTM STP 432, 1968, pp. 5-32.
17. B. Broberg to N.E. Hannerz and J.F. Lowery: "Influence of Micro Slag Distribution on MIG-MAG Weld Metal Impact Properties," *Metal Construction,* 1975, *7*(1), pp. 21-25.
18. K.-H. Schwalbe: "Processes at the Tip of a Statically Loaded Crack in AlZnMgCu0.5," *Int. J. Fracture Mech.,* 1972, *8,* pp. 456-57.
19. G.T. Hahn and A.R. Rosenfield, "Metallurgical Factors Affecting Fracture Toughness of Aluminum Alloys," *Metall. Trans.,* 1972, *6A,* pp. 653-68.
20. A.A. Wells: "Application of Fracture Mechanics at and Beyond General Yield," *Brit. Weld. J.,* 1963, *10,* pp. 563-70.
21. A.H. Cottrell: "Mechanics of Fracture in Large Structures," *Proc. Roy. Soc.,* 1965, *285,* pp. 10-21.
22. J.R. Rice: "Mathematical Analysis in the Mechanics of Fracture," in *Fracture: An Advanced Treatise,* H. Liebowitz, ed., 1968, Vol. II, pp. 233-248.
23. R.O. Ritchie and A.W. Thompson: "On Macroscopic and Microscopic Analyses for Crack Initiation and Crack Growth Toughness in Ductile Alloys," *Metall. Trans.,* 1985, *16A,* pp. 233-48.
24. J.N. Goodier and F.A. Field: "Plastic Energy Dissipation in Crack Propagation," in *Fracture of Solids,* D.C. Drucker and J.J. Gilman, ed., Gordon & Breach, New York, 1963, pp. 103-18.
25. A.L. Gurson: "Continuum Theory of Ductile Rupture by Void Nucleation and Growth," *J. Eng. Mater. Techol.,* 1977, *99,* pp. 2-15.
26. T. Pardoen and J.W. Hutchinson: "Micromechanics-Based Model for Trends in Toughness of Ductile Metals," *Acta Mater.,* 2003, *51,* pp. 133-48.
27. H.G.F. Wilsdorf: "The Ductile Fracture of Metals: A Microstructural Viewpoint," *Mater. Sci. Eng.,* 1983, *59,* pp. 1-59.